Inorganica Chimica Acta 407 (2013) 145–152

Contents lists available at ScienceDirect

Inorganica Chimica Acta

journal homepage: www.elsevier.com/locate/ica

Grafting of hydrophilic ethylene glycols or ethylenediamine on coordinatively unsaturated metal sites in MIL-100(Cr) for improved water adsorption characteristics

Martin Wickenheisser [a], Felix Jeremias [b], Stefan K. Henninger [b], Christoph Janiak [a,*]

[a] Institut für Anorganische Chemie und Strukturchemie, Universität Düsseldorf, 40204 Düsseldorf, Germany
[b] Dept. Thermally Active Materials and Solar Cooling, Fraunhofer Institute for Solar Energy Systems ISE, Heidenhofstr. 2, 79110 Freiburg, Germany

ARTICLE INFO

Article history:
Received 25 April 2013
Received in revised form 4 July 2013
Accepted 10 July 2013
Available online 23 July 2013

Keywords:
Metal–organic framework
Grafting
Ethylene glycols
Ethylenediamine
Water adsorption
Heat transformation

ABSTRACT

Grafting of activated MIL-100(Cr) with EG (ethylene glycol), DEG (diethylene glycol), TEG (triethylene glycol) and EN (ethylenediamine) leads to a decrease of the BET surface area and pore volume. Yet, water adsorption isotherms of the modified compounds MIL-100(Cr)-EG, MIL-100(Cr)-DEG and MIL-100(Cr)-EN show a favored uptake of water at lower partial pressures and no loss of total water uptake capacity compared to non-modified MIL-100(Cr). The reduction in surface area is offset by an increased hydrophilicity and an advantageous smaller pore size for the adsorption of water. MIL-100(Cr) is therefore very promising as a water sorption material, e.g., for heat-transformation applications.

© 2013 Elsevier B.V. All rights reserved.

1. Introduction

Since the past decade, tremendous research progress has been made in the utilization of metal organic frameworks (MOFs) [1–7], e.g., in gas storage [8–14], gas separation [8–10,15–20] and catalysis [21–26]. This class of compounds is based on metal clusters or metal ions linked by organic ligands forming a three-dimensional network possessing unique properties like huge surface areas and large pore volumes due to their tunable compositions. In recent years several groups have proposed that MOFs can be used as materials for reversible adsorption and desorption of water for possible use in heat transformation processes [27–36]. The basic principle for thermally driven adsorption chillers or heat pumps is shown in Fig. 1 [37,38]. The working fluid, e.g., water, is exchanged reversibly between the evaporator/condenser and the adsorbent, e.g., a MOF-material. The whole process can be split into a production and a regeneration cycle. During the production cycle (Fig. 1b) water is evaporated taking up evaporation enthalpy at a low temperature level. The evaporation enthalpy is useful cold in the cooling case, or taken from the environment during heat pump mode. The water vapor is then adsorbed in the porous material, releasing heat at a medium temperature level. The heat is used in the heat-pump case, or rejected to the environment during cooling mode. In the regeneration cycle (Fig. 1a) the saturated porous material is simply heated to release the adsorbed water. The required driving heat can be obtained at low cost, e.g., by a solar thermal facility, district heating, or excess heat from power-heat cogeneration plants. The water vapor is condensed at a medium temperature level and the heat of condensation is used or simply released to the environment in a cooling application [29].

Inorganic porous compounds like silica gels, aluminophosphates or zeolites have already been studied as water adsorbents for thermally driven adsorptions chillers or heat pump applications [39], but they have several disadvantages [40,41]. Zeolites have a high affinity to water and already adsorb at a low relative pressure of $P{\cdot}P_0^{-1} = 0.001–0.01$, but they require high desorption temperatures (typically over 300 °C) and have a low water loading lift [34]. Silica gels are less hydrophilic than zeolites which lead to lower desorption temperatures (typically approx. 100 °C) but also to a low water loading within the cycle [34]. Therefore, the development of new porous materials for water adsorption/desorption processes is an active research topic [37,38,41–43]. Purely inorganic materials like silica gels or zeolites are also not too versatile in terms of their chemical composition and tunable pore sizes compared to MOFs. Several MOFs have already shown higher water uptake capacities

* Corresponding author. Tel.: +49 2118112286.
E-mail addresses: stefan.henninger@ise.fraunhofer.de (S.K. Henninger), janiak@uni-duesseldorf.de (C. Janiak).

0020-1693/$ - see front matter © 2013 Elsevier B.V. All rights reserved.
http://dx.doi.org/10.1016/j.ica.2013.07.024

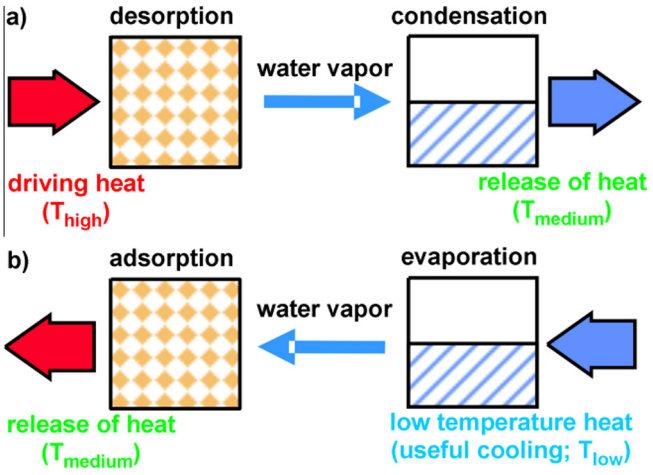

Fig. 1. Basic principle for thermally driven adsorption chillers or heat pumps [29].

with very promising water sorption characteristics like the MIL-100 [30,32,44] and MIL-101 [31,35,36,45] compounds (MIL stands for Materials of Institute Lavoisier [46,47]) [29,34,48]. MIL-100 has the empirical formula $\{M_3(\mu_3\text{-}O)(X)(H_2O)_2(BTC)_2 \cdot nH_2O\}_n$ (M = Cr [49], Fe [50], Al [51]; X = OH, F; BTC = 1,3,5-benzene tricarboxylate) (Fig. 2). These three isostructural compounds possess two types of mesopores with cages of 25 and 29 Å in diameter (Fig. 2c).

The water sorption characteristics of native MIL-100(Cr) have been investigated by Kitagawa et al. with a water uptake of 0.60 g g^{-1} at a moderate humidity ($P \cdot P_0^{-1} < 0.6$) [30]. The high internal surface area and a good hydrothermal stability (stable over 2000 water ad-/desorption cycles) make MIL-100(Cr) a promising material for heat transformation processes [30]. For the intended application however, the water uptake in a relative pressure window of $0.05 < P \cdot P_0^{-1} < 0.32$ has to be maximized [34,37]. Shifting the water adsorption curves of porous, hydrophilic compounds to lower relative pressure is connected with increasing the hydrophilicity of this material. Stock et al. realized a post-synthetic modification of MIL-101(Cr) by introducing hydrophilic groups like $-NO_2$ or $-NH_2$ directly at the linker molecule [36,52,53]. Both compounds and another "$-SO_3H$ modified" version of MIL-101(Cr) were investigated by Kitagawa and co-workers in terms of their water sorption behavior [35]. Two of these modified materials have shown an increased hydrophilicity, which means that the loading step of the corresponding adsorption isotherms were shifted by $P \cdot P_0^{-1} = 0.05$ to lower relative pressure compared to the native MIL-101(Cr) compound [35,36].

A second possibility to increase the hydrophilicity of MOFs can be realized by creating a coordinative metal–ligand interaction, as described by Cohen and Wang [52]. The group of Ferey et al. modified MIL-101(Cr) by grafting with ethylenediamine, diethylenetriamine and 3-aminopropyltrialkoxysilane directly at the chromium oxidocluster. Cr(III) octahedral clusters of MIL-100(Cr) possess terminal water molecules (Fig. 2a, Fig. 2b), which can be removed by vacuum treatment of the material at 473 K, generating the coordinatively unsaturated metal sites (CUS) available and usable for post-synthetic modifications [54]. In the case of MIL-101(Cr) and MIL-100(Fe) approximately 3 and 2 mmol g^{-1} of free CUS, respectively, can be generated [54]. Successful grafting experiments are reported for MIL-100(Cr) (in which the CUS have been grafted with CO, CD_3OH, CF_3CH_2OH and $(CF_3)_2CHOH$) [55] for MIL-100(Fe) [56] MIL-100(Al) [57] and MIL-101(Cr) [54].

In this work we present the grafting of MIL-100(Cr) (Fig. 2) with hydrophilic ethylene glycol (EG), diethylene glycol (DEG), triethylene glycol (TEG) and ethylenediamine (EN) (Scheme 1) to study their water sorption characteristics.

2. Experimental

2.1. Materials and methods

All chemicals were obtained commercially and were used without further purification: 1,3,5-benzenetricarboxylic acid (H_3BTC) (Alfa Aesar, 98%); hydrofluoric acid (Acros Organics, 48–51% in water); CrO_3 (Alfa Aesar, 99%); ethylene glycol (EG) (Janssen Chimica, >99%); diethylene glycol (DEG) (Sigma–Aldrich, >99%); triethylene glycol (TEG) (J.T. Baker, 99%); ethylenediamine (EN) (Alfa Aesar, 99%); D_2O/NaOD (40 wt.% NaOD in D_2O) (Sigma–Aldrich, 99.9%); toluene (VWR, p.a.); DMF (VWR, p.a.), ethanol (VWR, p.a.). Toluene was additionally dried over molecular sieve (4 Å) before usage leading to a water content of 0.015 wt.% (determined by Karl Fischer titration). Post-synthetic modification reactions were carried out under nitrogen atmosphere. Filtration, centrifugation and washing of the crude products were performed with exposure to air.

2.2. Physical measurements

Powder X-ray diffraction (PXRD) patterns of all the samples were measured at ambient temperature on a Bruker D2 Phaser using a flat sample holder and Cu Kα radiation ($\lambda = 1.54182$ Å). Diffractograms were obtained on flat layer sample holders where at low angle the beam spot is strongly broadened so that only a fraction of the reflected radiation reaches the detector which leads to the low relative intensities measured at $2\theta < 7°$. FT-IR measurements were carried out on a Bruker TENSOR 37 IR spectrometer at ambient temperature in a range of 4000–500 cm^{-1} either in a KBr disk or on a diamond ATR unit. Nitrogen physisorption isotherms were measured on a Quantachrome Nova 4000e at 77 K. Water physisorption isotherms were measured volumetrically on a Quantachrome Autosorb iQ MP at 293 K. All samples were activated and vacuum-degassed before nitrogen and water sorption measurements for 2–4 h at 473 K. The samples were transferred to a pre-weighed sample tubes capped with a septum. Then the sample tube was connected to the preparation port of the sorption analyzer and degassed under vacuum for the specified time and temperature. After weighing, the sample tube was then transferred to the analysis port of the sorption analyzer. Helium gas was used for the determination of the cold and warm free space of the sample tubes. DFT calculations for the pore size distribution curves were carried out with the native ASIQWIN 1.2 software employing the 'N_2 at 77 K on carbon, slit pore, NLDFT equilibrium' model [58–60]. The water cycling measurement was performed in a Setaram TG-DSC 111, where samples were exposed to an Ar flow humidified by a Setaram WetSys. Solution NMR spectra were recorded on a Bruker Avance DRX200 operating at 200 MHz for ^1H (see Supplementary data for details).

2.3. Synthesis of MIL-100(Cr)

MIL-100(Cr) was hydrothermally synthesized according to the literature [44]. Typical batch sizes of 1.20 g (12.0 mmol) CrO_3, 2.52 g (12.0 mmol) H_3BTC and 0.42 mL hydrofluoric acid (12 mmol; 48–51% HF in H_2O) in water (58 mL) at 473 K for 4 days yielded MIL-100(Cr)-as synthesized. For activation the as-synthesized material was purified through stepwise washing procedures with DMF, EtOH and deionized water (see Supplementary data for details). An amount of 2.65 g of the purified MIL-100 was obtained (60% yield based on Cr) as a light green powder with a BET surface of 1330 $m^2 g^{-1}$ and a pore volume of 0.77 $cm^3 g^{-1}$ (measured at $P \cdot P_0^{-1} = 0.95$) (cf. Table 2).

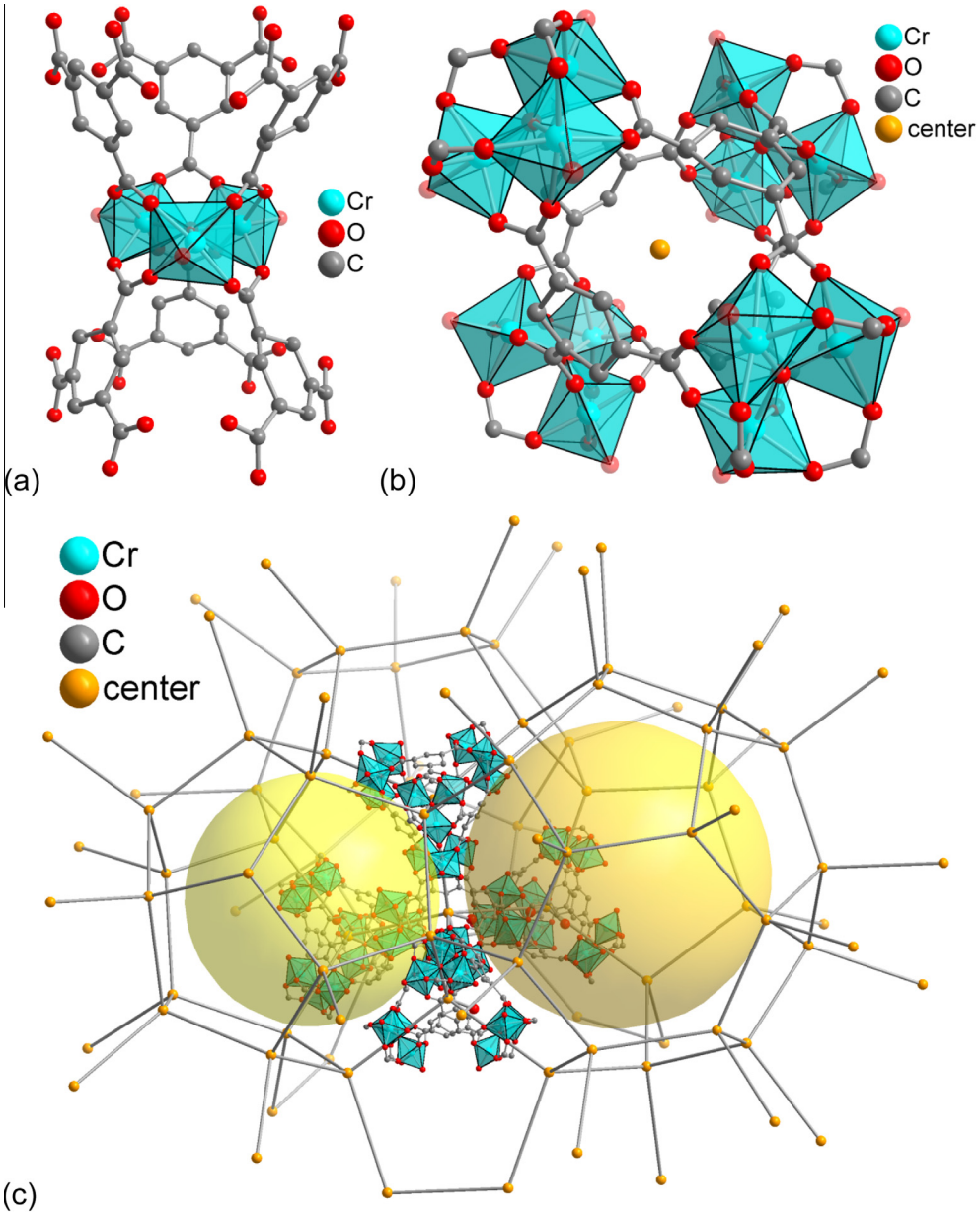

Fig. 2. (a) Secondary building unit, (b) single supertetrahedra with indicated center, (c) polygons for small S cage and large L cage in MIL-100(Cr) formed by connecting the centers of the corner-sharing supertetrahedra (different objects are not drawn to scale). The transparent yellow spheres of diameter 25 Å (left) and 29 Å (right) depict the void space in the cages. In (a) and (b) the O-atoms of the removable aqua ligands at the Cr octahedra are shown semi-transparent. Hydrogen atoms and solvent molecules of crystallization are not shown (redrawn from deposited cif-file to CCDC number 648835).

2.4. Reactions of EG, DEG, TEG and EN with activated MIL-100(Cr)

The purified, solid MIL-100(Cr) material (100 mg) was placed in a two-necked flask and degassed for at least 1 h in vacuum at 473 K to remove any adsorbed water or solvent from the metal sites, thus generating the coordinatively unsaturated sites (CUS) according to the literature [44]. After cooling to r.t., dry toluene was added to the activated solid. Then pure, neat (mono, di- or tri-)ethylene glycol or ethylenediamine was added dropwise to the suspensions. The reaction mixtures were stirred for at least 16 h at r.t. (EN) or at 373 K (EG, DEG, TEG). The crude products were isolated by filtration and purified by removing the excessive glycols or amines by washing with acetone (see Supplementary data for details).

3. Results and discussion

3.1. Syntheses of ethylene glycol and ethylenediamine grafted MIL-100(Cr)

The synthesis of the EG-, DEG-, TEG- and EN-grafted MIL-100(Cr) materials with (mono, di- or tri-)ethylene glycol and ethylenediamine, respectively, was carried out by stirring activated MIL-100(Cr) with the substrate molecules in dry toluene for at least 16 h at r.t. (EN) or at 373 K (EG, DEG, TEG). The unchanged X-ray diffraction patterns of the isolated, modified compounds MIL-100(Cr)-EG, MIL-100(Cr)-DEG, MIL-100(Cr)-TEG and MIL-100(Cr)-EN show no loss of crystallinity compared to native MIL-100(Cr) (Fig. 3).

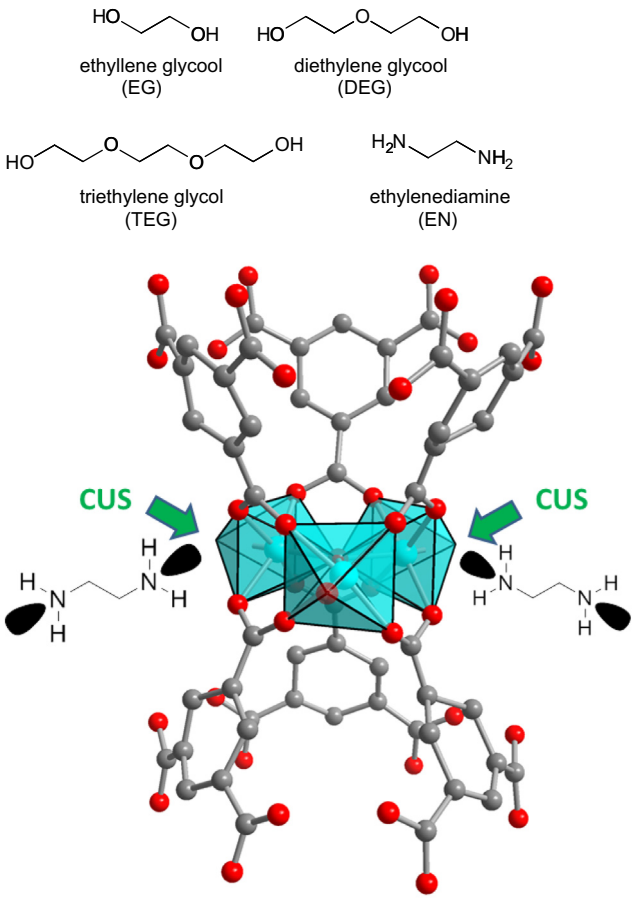

Scheme 1. Molecules used for grafting of MIL-100(Cr) and schematic illustration of addition (grafting) of EN to coordinatively unsaturated metal sites (CUS) at the secondary building unit of MIL-100(Cr) (cf. Fig. 2).

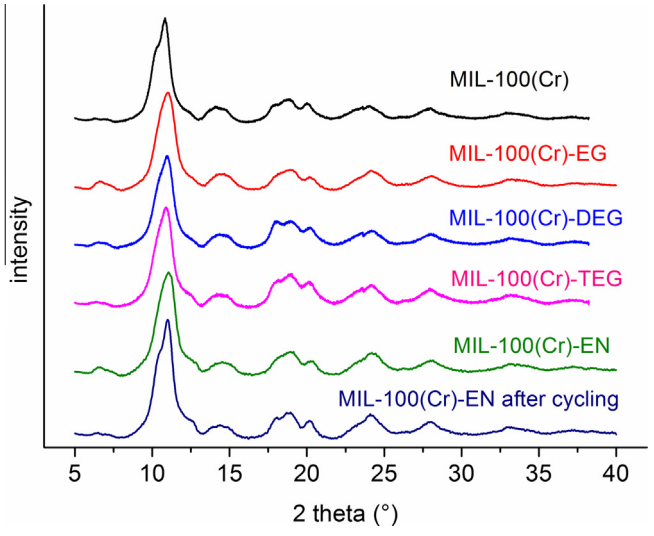

Fig. 3. PXRD patterns of native MIL-100(Cr) and EG-, DEG-, TEG- and EN-modified MIL-100(Cr). The PXRD for MIL-100(Cr)-EN is given before and after water sorption cycling (bottom-two curves).

Infrared spectra of ethylene glycol-modified MIL-100(Cr) prove the presence of the glycols EG, DEG and TEG by the new ν(C–H)– and ν(C–O)-stretching vibrations at 2959–2877 cm^{-1} (ν(C–H)) and 1123–1042 cm^{-1} (ν(C–O)), respectively (Fig. 4a). The ν(C–H)-stretching vibrations are shifted to larger wavenumbers by

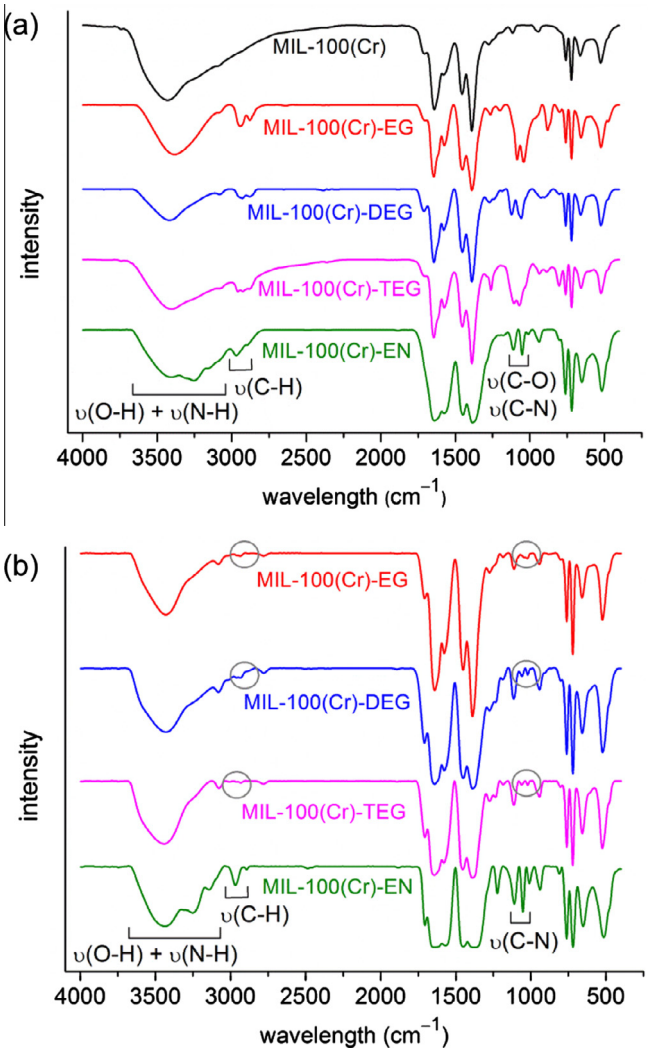

Fig. 4. (a) IR-spectra (KBr) of activated native MIL-100(Cr) and EG-, DEG-, TEG- and EN-modified MIL-100(Cr) obtained by reaction of activated MIL-100(Cr) with the glycols and EN in toluene. (b) IR-spectra (KBr) of isolated reaction products of MIL-100(Cr) treated first with water, then with the grafting reagents (EG, DEG, TEG, EN). The grey circles highlight the areas of the missing aliphatic ν(C–H)– and ν(C–O)-stretching vibrations for the glycols (cf. Fig. 4a).

3–9 cm^{-1} compared to the free ligands (see Table S1 in Supplementary data for details). This shift can be observed when a ligand is coordinated to a Lewis acidic center [61,62], therefore indicating the successful grafting of EG, DEG and TEG onto chromium(III) sites. The presence of EN in MIL-100(Cr) is proven by the IR-spectrum (Fig. 4a), showing shoulders in the area of 3700–2600 cm^{-1}, which can be assigned to ν(N–H)-valence vibrations. Aliphatic ν(C–H)-vibration bands of coordinated EN are shifted to larger wavenumbers compared to the free EN ligand (44–47 cm^{-1}) (see Table S1 for details), indicating a coordination onto the Lewis acid chromium centers [61,62]. The band at 1053 cm^{-1} can be assigned to a ν(C–N)-stretching vibration of coordinated EN.

To further verify coordination of glycols and ethylenediamine to the chromium center, the activated MIL-100(Cr) compound was first soaked with water to ensure that the coordinative unsaturated metal sites were occupied by water molecules, followed by an intensive treatment with EG, DEG, TEG or EN (see Supplementary data for details). IR-spectra of the compounds treated this way show only almost invisible, that is, barely detectable bands of low intensity for aliphatic ν(C–H)– and ν(C–O)-stretching vibrations in the region of 2900–3000 cm^{-1} and 1150–1000 cm^{-1},

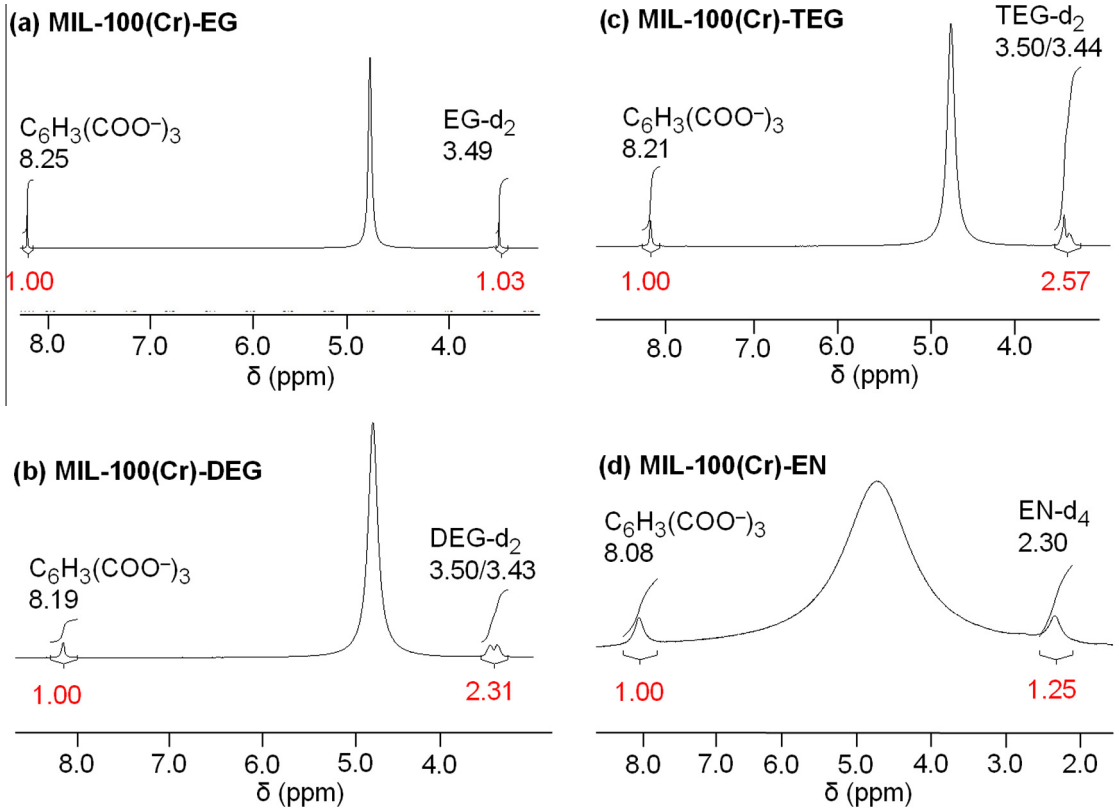

Fig. 5. ^{1}H NMR spectra (200 MHz) of the organic components in D_2O/NaOD solution after decomposition of (a) MIL-100(Cr)-EG, (b) MIL-100(Cr)-DEG, (c) MIL-100(Cr)-TEG and (d) MIL-100(Cr)-EN in D_2O/NaOD (40 wt.% of NaOD in D_2O) with the relative intensities (in red) and assignments of individual (pH dependent) resonances. The solvent signals D_2O were set to δ = 4.79 ppm. (For interpretation of the references to colour in this figure legend, the reader is referred to the web version of this article.)

respectively (Fig. 4b). This indicates that a possible exchange of aqua ligands by glycol ligands occurs only to an insignificant extent. As a result is can be stated that grafting of MIL-100(Cr) with glycols requires vacant Cr(III) sites for coordination. However, the IR-spectrum of the EN-modified compound, obtained after water treatment, shows bands for aliphatic ν(C–H)-stretching vibrations at 2968 and 2892 cm^{-1} (Fig. 4b) as before in Fig. 4a. This indicates that aqua ligands were exchanged by EN due to the larger nucleophilicity of the latter.

3.2. Quantification of grafting reagents by NMR-spectroscopy

To determine quantitatively the amount of grafted EG, DEG, TEG and EN, the modified MILs were hydrolyzed in D_2O/NaOD (see Supplementary data for details). ^{1}H NMR spectra were recorded of the supernatant solution after hydrolysis and show signals of the deprotonated and deuterium exchanged ligand $C_6H_3(COO^-)_3$ ligand (BTC^{3-}) and the grafting reagents (EG-d_2, DEG-d_2, TEG-d_2, EN-d_4) (Fig. 5).

The amounts of grafted EG, DEG, TEG and EN in MIL-100(Cr) range from 0.64 to 0.94 for the molar BTC to graft molecule ratio and 0.43 to 0.63 for the molar Cr: graft ratio (Table 1).

3.3. N_2-sorption studies

Successful grafting explains the decrease in BET surface from N_2-sorption measurements. The BET surfaces of the modified compounds MIL-100(Cr)-EG, MIL-100(Cr)-DEG, MIL-100(Cr)-TEG and MIL-100(Cr)-EN are reduced to approximately 50% compared to the BET surface area of non-modified MIL-100(Cr). With the BET surface also the available pore volume is reduced (Table 2).

Table 1
Amount of graft reagent in modified MIL-100(Cr).

Graft reagent	MIL-100(Cr)			
	-EG	-DEG	-TEG	-EN
Molar ratio[a] BTC:graft reagent	1:0.77	1:0.87	1:0.64	1:0.94
Molar ratio[b] Cr:graft reagent	1:0.51	1:0.58	1:0.43	1:0.63
wt.% Graft reagent[c]	13.6%	23.4%	24.1%	15.7%

[a] Determined from ^{1}H NMR integrals of aromatic H atoms of $C_6H_3(COO^-)_3$ ligand and aliphatic CH_2 groups of grafting reagents (EG-d_2, DEG-d_2, TEG-d_2, EN-d_4), see Fig. 5. The NMR proton ratio takes into account the different proton number of the $C_6H_3(COO^-)_3$ linker (3 H atoms), EG (4), DEG (8), TEG (12) and EN (4 H atoms).

[b] Calculated based on the molar ratio of 3:2 for Cr and BTC ligand in $\{Cr_3(\mu_3\text{-}O)(F)(BTC)_2\}$ ($C_{18}H_6Cr_3FO_{13}$, 605.231 g mol^{-1}).

[c] $w(x) = \frac{m(\text{graft})}{m(\text{graft})+m(\text{MIL-100})}$, Calculated based on the molar masses (g mol^{-1}) of EG (62.07), DEG (106.12), TEG (150.17) and EN (60.10).

The pore size distribution curves indicate that non-modified MIL-100(Cr) possesses two different kinds of pores with average pore diameters of 15 and 26 Å, respectively (Fig. 6). Possibly due to retained impurities the average diameters of both pores are smaller than expected (25 and 29 Å, cf. Fig. 2) [49,50]. Grafting of MIL-100(Cr) with EG, DEG and TEG leads to at least three different kinds of pores with diameters varying around 12, 15 and 19 Å. In the case of MIL-100(Cr)-DEG, a small fraction of the pores seems to remain unaltered with a pore diameter of 26 Å. Filling of the larger pores of 26 Å probably leads to the reduced pore size of about 19 Å. The smaller pores of MIL-100(Cr) (15 Å diameter) are mostly transformed to pores with a diameter of about 12 Å in all three cases. Grafting of MIL-100(Cr) with EN leads to five type of pores with diameters of 12, 15, 19, 23 and 26 Å (Fig. 6). Filling of the

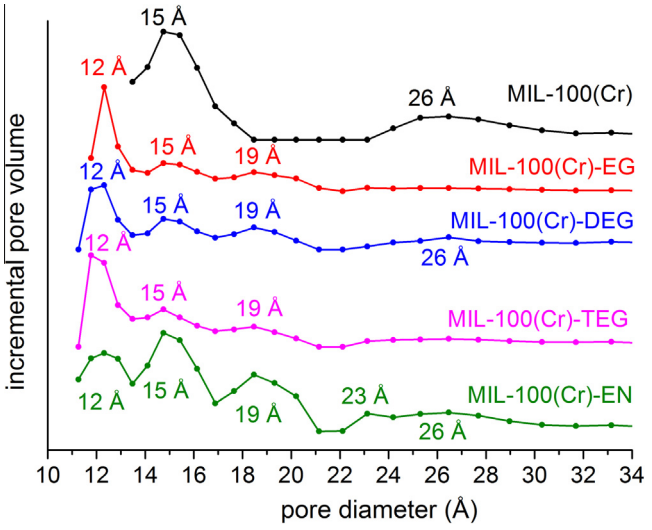

Fig. 6. Pore size distribution curves of non-modified MIL-100(Cr) and EG-, DEG-, TEG- and EN-modified MIL-100(Cr).

larger pores (26 Å) with EN mostly leads to the reduced pore sizes of 19 and 23 Å with a residual amount of original pores (26 Å). The smaller pores of MIL-100(Cr) (15 Å) are again partially transformed into pores with a diameter of ~12 Å.

3.4. Water sorption studies

Water adsorption isotherms of MIL-100(Cr)-EG, MIL-100(Cr)-DEG, MIL-100(Cr)-TEG and MIL-100(Cr)-EN are shown in comparison to the adsorption isotherm of the native MIL-100(Cr) (Fig. 7). Water loading values are included in Table 2. The water sorption isotherm of MIL-100(Cr) has been investigated in detail before [30].

Despite the reduction of the BET surfaces of grafted MIL-100(Cr) by about or more than 50% compared to non-modified MIL-100(Cr) (see Table 2), the water loadings remain comparatively high (Fig. 7, Table 2). The EG- and DEG-modified samples even have slightly higher water uptake capacities, compared to native MIL-100(Cr). However, the increase in the water adsorption isotherm near $P{\cdot}P_0^{-1} = 1$ may be due to a water condensation effect, which can occur close to the dew point of water [63,64]. The water uptake capacity is not only determined by the available porosity, but also by the hydrophobicity/hydrophilicity of the ligand, the hydrogen-bonding capabilities, directing and interference effects of functional groups, site preference and a possible degradation or structure transition of the adsorbent material [65]. The inverse relation of the pore size distribution and the water adsorption capacity was tried to understand by infrared spectroscopy and N_2-sorption studies of the compounds after water sorption measurements. The IR-spectra of the four grafted samples show that MIL-100(Cr)-EG loses part of the coordinated EG. Coordinated DEG, TEG and EN is still visible in the IR-spectra and their ν(C–H)– and ν(C–O)– or ν(C–N)-bands show only a slight decrease in their intensities (Fig. S4b, Fig. S7). The BET surface areas of the grafted samples, recorded after water sorption measurements, are only slightly increased compared to the surface areas measured before (Table 2). Both studies agree that only a small part of EG, DEG, TEG and EN is removed through the water sorption measurements. The high water uptakes together with the reduction of the surface areas can only be explained by the fact that the sizes of the pores are not the crucial factor for a high amount of adsorbed water. The chemical alteration of the MOF material after modification seems to dominate the water uptake capacities.

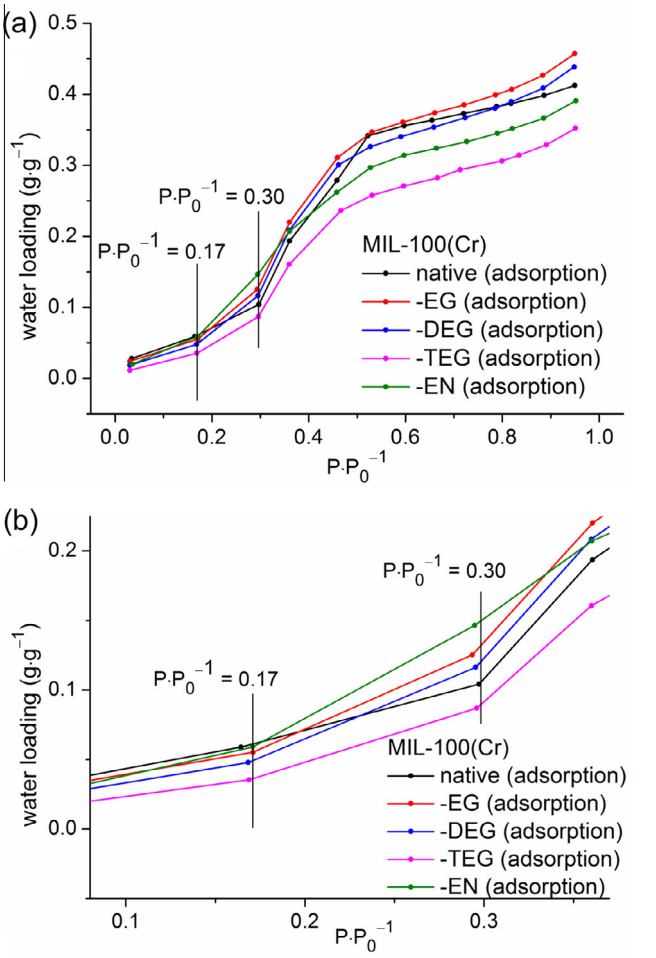

Fig. 7. (a) Water adsorption isotherms of non-modified MIL-100(Cr) and EG-, DEG-, TEG- and EN-modified MIL-100(Cr) at 293 K. (b) Enlargement for region $0.10 < P{\cdot}P_0^{-1} < 0.35$.

Table 2
Nitrogen and water adsorption measurements.

Compound	BET surface area ($m^2\ g^{-1}$) of activated material[a]	Total pore volume ($cm^3\ g^{-1}$)[b]	max. water loading ($g\ g^{-1}$ at 20 °C)[c]	BET surface area ($m^2\ g^{-1}$) after water sorption[d]
MIL-100(Cr)	1330	0.77	0.40	–
MIL-100(Cr)-EG	710	0.47	0.43	800
MIL-100(Cr)-DEG	580	0.50	0.42	720
MIL-100(Cr)-TEG	680	0.53	0.33	700
MIL-100(Cr)-EN	640	0.42	0.37	690 [d], 700 [e]

[a] BET surface area calculated at $0.05 < P{\cdot}P_0^{-1} < 0.2$ from N_2 sorption isotherm at 77 K with a standard deviation of ± 20 m^2/g.
[b] Calculated from N_2 sorption isotherm at 77 K ($P{\cdot}P_0^{-1} = 0.95$) for pores ⩽20 nm.
[c] Calculated from water sorption isotherm at 293 K ($P{\cdot}P_0^{-1} = 0.9$).
[d] After single water sorption experiment.
[e] After 20 water sorption cycle experiments.

The samples MIL-100(Cr)-EG, MIL-100(Cr)-DEG and MIL-100(Cr)-EN exhibit even a slightly favored water uptake compared to MIL-100(Cr) due to the higher slope of the adsorption isotherms of the modified compounds in comparison to MIL-100(Cr) in a region of $0.17 < P{\cdot}P_0^{-1} < 0.30$ (Fig. 7a and b). This proof of concept demonstrates that it is possible to shift the water adsorption isotherms to lower relative pressure by grafting hydrophilic groups onto coordinatively unsaturated metal sites.

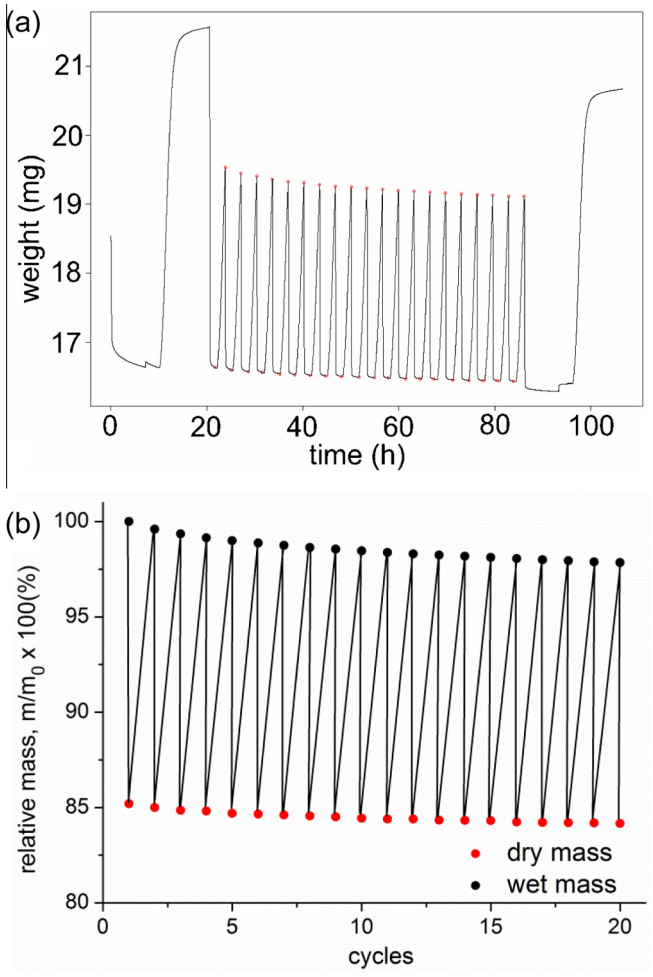

Fig. 8. (a) Water load signal and (b) relative mass variation of MIL-100(Cr)-EN during water desorption and adsorption over 20 cycles acquired at p_{H2O} = 5.6 kPa. In (b) the initial mass m_0 with adsorbed water is set to 100% and the subsequent masses related thereupon as $m/m_0 \times 100\%$

A porous sorption material for thermally driven adsorptions chillers or heat pump applications should show a high water uptake capacity in between $0.05 < P{\cdot}P_0^{-1} < 0.32$ relative pressure range, that is, at low to medium humidity. With regard to the performance at low to medium water partial pressure, an adsorption/desorption cycle stability test of the promising MIL-100(Cr)-EN was performed, monitoring the loading of the sample by thermogravimetry (Fig. 8). The EN-grafted MIL-100(Cr) was chosen for the cycle stability test due to the higher stability of the Cr–EN coordinative bond compared to the Cr–glycol bond. The sample has been exposed to a humidified gas flow in a short cycle test consisting of a continuous cycling between 140 and 40 °C over 20 cycles under a constant partial water vapor pressure of 5.6 kPa using argon as a carrier and 4 h per cycle. As the heat of adsorption is poorly dissipated in the cycling experiments, kinetics is slow and absolute equilibrium is reached only in the long analytic cycles at the beginning and in the end of the experiment (Fig. 8a). The change of total mass variation during water desorption and adsorption is shown in Fig. 8, which indicates a total (dry) mass loss of 1.7%. Compared to non-grafted MOFs like MIL-100(Fe) and MIL-100(Al) (Δ dry mass loss = 0.6% (Fe), 1.4% (Al)) the mass loss of EN-grafted MIL-100(Cr) is only slightly increased [33]. Water loading capacities were measured before and after the cycles. The total water loading loss of 10.8% the long analytic cycles at the beginning and in the end of the experiment (Fig. 8a) indicates some sort of degradation. This degradation of MIL-100(Cr)-EN is higher than in MIL-101(Cr) (−1.9%) [31], MIL-100(Fe) (−3.0%) and MIL-100(Al) (−4.5%) [33]. The increased mass and water loading loss could be explained due to a partial loss of grafted ethylenediamine. The partial loss of EN is supported by the loss in dry mass. The results of the cycling stability test are summarized in Table 3.

Table 3
Results of water cycling stability test of MIL-100(Cr)-EN.

	Before cycling	After cycling	Δ (%)
Dry mass (mg)	16.64	16.35	−1.7
Water loading ($g\,g^{-1}$)	0.296	0.264	−10.8
BET surface ($m^2\,g^{-1}$)	640	700	+9.4

Powder X-ray diffraction, infrared-spectroscopy and BET measurements were carried out after 20 cycles. There is no significant change in crystallinity (Fig. 3). The IR-spectrum appears almost unchanged (Fig. S7) and the BET-surface increases from 640 $m^2\,g^{-1}$ before to 700 $m^2\,g^{-1}$ after 20 water cycles (Table 2). This BET surface increase of 9.4% may be due to a partial loss of coordinated ethylenediamine, concomitant with the decrease in dry mass. Long-time measurements will have to prove the stability of MIL-100(Cr)-EN after a large number of cycles. Regarding possible practical applications, the use of EN-grafted MIL-100 has to be critically evaluated due to the partial loss of EN as evidenced by BET- and water loading measurements before and after 20 water adsorption–desorption cycles. Cycling experiments with an even larger number of water cycles still have to evaluate the practical use of this new compound.

4. Conclusions

We presented the grafting of coordinatively unsaturated metal sites (CUS) in MIL-100(Cr) with EG, DEG, TEG and EN characterized by IR-spectroscopy and N_2-sorption measurements. The slope of the water adsorption isotherms of MIL-100(Cr)-EG, MIL-100(Cr)-DEG and MIL-100(Cr)-EN in the $0.17 < P{\cdot}P_0^{-1} < 0.30$ is increased, compared to native MIL-100(Cr). This means that water uptake in the modified materials is favored in this partial pressure region for thermally driven adsorptions chillers or heat pump applications which should show a high water uptake capacity in between $0.05 < P{\cdot}P_0^{-1} < 0.32$ relative pressure range, that is, at low to medium humidity. In spite of the fact that the modifications of MIL-100(Cr) lead to materials with reduced pore sizes, the total water uptake capacities remain high. Water adsorption capacity correlates with the available pore volume and the hydrophobicity/hydrophilicity of the ligand, the hydrogen-bonding capabilities and directing effects of functional groups, site preference and a possible degradation or structure transition. The increased hydrophilicity of the MOF material after modification seems to dominate the water uptake capacities. Further, smaller pores can be advantageous for earlier water adsorption and condensation [30,33]. Despite the different interaction between MOFs and active carbon or AlPOs with water smaller pores in the range of 6–10 Å known from active carbon and AlPOs might be preferable also in case of MOFs for earlier water adsorption [66].

This proof-of-concept illustrates and opens the possibility to fine-tune the water adsorption characteristics based on well-investigated stable MOFs without linker or post-synthetic linker modification by simple addition (grafting) of terminal ligands to free metal sites or exchange of terminal aqua ligands at the metal sites. An amine ligand has shown more stable binding to Cr(III) over alcohol ligands and more amine ligands will be investigated in more detail for the grafting of MIL-100(Cr) and MIL-101(Cr).

Acknowledgement

Funding by the Federal of Economics (BMWi) under Grant 0327851A/B is gratefully acknowledged.

Appendix A. Supplementary material

Supplementary data associated with this article can be found, in the online version, at http://dx.doi.org/10.1016/j.ica.2013.07.024.

References

[1] J.R. Long, O.M. Yaghi, Chem. Soc. Rev. 38 (2009) 1213.
[2] K. Biradha, M.J. Zaworotko, New J. Chem. 34 (2010) 2353.
[3] S. Kitagawa, S. Natarajan, Eur. J. Inorg. Chem. 24 (2010) 3685.
[4] C. Janiak, Dalton Trans. 14 (2003) 2781.
[5] C. Janiak, J.K. Vieth, New J. Chem. 34 (2010) 2366.
[6] A.U. Czaja, N. Trukhan, U. Müller, Chem. Soc. Rev. 38 (2009) 1284.
[7] U. Müller, M. Schubert, F. Teich, H. Pütter, K. Schierle-Arndt, J. Pastré, J. Mater. Chem. 16 (2006) 626.
[8] (a) H. Wu, Q. Gong, D.H. Olson, J. Li, Chem. Rev. 112 (2012) 836;
(b) K. Li, D.H. Olson, J. Li, Inorg. Chem. 12 (2010) 13.
[9] (a) L.J. Murray, M. Dinca, J.R. Long, Chem. Soc. Rev. 38 (2009) 1294;
(b) R.E. Morris, P.S. Wheatley, Angew. Chem., Int. Ed. 47 (2008) 4966.
[10] J.-R. Li, R.J. Kuppler, H.-C. Zhou, Chem. Soc. Rev. 38 (2009) 1477.
[11] (a) M. Paik Suh, Y.E. Cheon, E.Y. Lee, Coord. Chem. Rev. 252 (2008) 1007;
(b) C.J. Kepert, Chem. Commun. 7 (2006) 695.
[12] M. Paik Suh, H.J. Park, T.K. Prasad, D.-W. Lim, Chem. Rev. 112 (2012) 782.
[13] (a) T. Düren, Y.-S. Bae, R.Q. Snurr, Chem. Soc. Rev. 38 (2009) 1237;
(b) S.S. Han, J.L. Mendoza-Cortés, W.A. Goddard, Chem. Soc. Rev. 38 (2009) 1460;
(c) R.B. Getman, Y.-S. Bae, C.E. Wilmer, R.Q. Snurr, Chem. Rev. 112 (2012) 703.
[14] (a) Z. Chen, S. Xiang, H.D. Arman, P. Li, S. Tidrow, D. Zhao, B. Chen, Eur. J. Inorg. Chem. 24 (2010) 3745;
(b) F. Ma, S. Liu, D. Liang, G. Ren, C. Zhang, F. Wei, Z. Su, Eur. J. Inorg. Chem. 24 (2010) 3756.
[15] Z. Zhang, Y. Zhao, Q. Gong, Z. Li, J. Li, Chem. Commun. 49 (2013) 653.
[16] (a) J.-R. Li, Y. Ma, M.C. McCarthy, J. Sculley, J. Yu, H.-K. Jeong, P.B. Balbuena, H.-C. Zhou, Coord. Chem. Rev. 255 (2011) 1791;
(b) J.-R. Li, J. Sculley, H.-C. Zhou, Chem. Rev. 112 (2012) 869.
[17] D. Liu, C. Zhong, J. Mater. Chem. 20 (2010) 10308.
[18] G. Férey, C. Serre, T. Devic, G. Maurin, H. Jobic, P.L. Llewellyn, G. De Weireld, A. Vimont, M. Daturi, J.-S. Chang, Chem. Soc. Rev. 40 (2011) 550.
[19] (a) S.K. Nune, P.K. Thallapally, B.P. McGrail, J. Mater. Chem. 20 (2010) 7623;
(b) G.-P. Hao, W.-C. Li, A.-H. Lu, J. Mater. Chem. 21 (2011) 6447.
[20] (a) H.B. Tanh Jeazet, C. Staudt, C. Janiak, Dalton Trans. 41 (2012) 14003;
(b) B. Zornoza, C. Tellez, J. Coronas, J. Gascon, F. Kapteijn, Microporous Mesoporous Mater. 166 (2013) 67;
(c) D. Bastani, N. Esmaeili, M. Asadollahi, J. Ind. Eng. Chem. 19 (2013) 375;
(d) G. Dong, H. Li, V. Chen, J. Mater. Chem. A 1 (2013) 4610.
[21] M. Yoon, R. Srirambalaji, K. Kim, Chem. Rev. 112 (2012) 1196.
[22] D. Farrusseng, S. Aguado, C. Pinel, Angew. Chem., Int. Ed. 48 (2009) 7502.
[23] J. Lee, O.K. Farha, J. Roberts, K.A. Scheidt, S.T. Nguyen, J.T. Hupp, Chem. Soc. Rev. 38 (2009) 1450.
[24] L. Ma, C. Abney, W. Lin, Chem. Soc. Rev. 38 (2009) 1248.
[25] T. Ladrak, S. Smulders, O. Roubeau, S.J. Teat, P. Gamez, J. Reedijk, Eur. J. Inorg. Chem. 24 (2010) 3804.
[26] W. Kleist, F. Jutz, M. Maciejewski, A. Baiker, Eur. J. Inorg. Chem. 24 (2009) 3552.
[27] Yu.I. Aristov, J. Chem. Eng. Jpn. 40 (2007) 1241.
[28] E. Biemmi, A. Darga, N. Stock, T. Bein, Microporous Mesoporous Mater. 114 (2008) 380.
[29] S.K. Henninger, H.A. Habib, C. Janiak, J. Am. Chem. Soc. 131 (2009) 2776.
[30] G. Akiyama, R. Matsuda, S. Kitagawa, Chem. Lett. 39 (2010) 360.
[31] J. Ehrenmann, S.K. Henninger, C. Janiak, Eur. J. Inorg. Chem. 4 (2011) 471.
[32] J.-P. Zhang, A.-X. Zhu, R.-B. Lin, X.-L. Qi, X.-M. Chen, Adv. Mater. 23 (2011) 1268.
[33] F. Jeremias, A. Khutia, S.K. Henninger, C. Janiak, J. Mater. Chem. 22 (2012) 10148.
[34] (a) C. Janiak, S.K. Henninger, Chimia 67 (2013) 754;
(b) S.K. Henninger, F. Jeremias, H. Kummer, C. Janiak, Eur. J. Inorg. Chem. 16 (2012) 2625.
[35] G. Akiyama, R. Matsuda, H. Sato, A. Hori, M. Takata, S. Kitagawa, Microporous Mesoporous Mater. 157 (2012) 89.
[36] (a) A. Khutia, H.U. Rammelberg, T. Schmidt, S. Henninger, C. Janiak, Chem. Mater. 25 (2013) 1235;
(b) F. Jeremias, V. Lozan, S. Henninger, C. Janiak, Dalton Trans. (2013) in press, Doi: http://dx.doi.org/10.1039/C3DT51471D.
[37] (a) Yu.I. Aristov, Appl. Therm. Eng. 50 (2013) 1610;
(b) A. Hauer, Adsorption 13 (2007) 399;
(c) T. Núñez, W. Mittelbach, H.-M. Henning, Appl. Therm. Eng. 27 (2007) 2205.
[38] (a) S.K. Henninger, F. Jeremias, H. Kummer, P. Schossig, H.-M. Henning, Energy Procedia 30 (2012) 279;
(b) H. Demira, M. Mobedi, S. Ülkü, Renewable Sustainable Energy Rev. 12 (2008) 2381;
(c) Yu.I. Aristov, B. Dawoud, I.S. Glaznev, A. Elyas, Int. J. Heat Mass Transfer 51 (2008) 4966;
(d) H.-M. Henning, Appl. Therm. Eng. 27 (2007) 1734.
[39] (a) Yu.I. Aristov, Int. J. Refrig. 32 (2009) 675;
(b) B.B. Saha, A. Chakraborty, S. Koyama, Yu.I. Aristov, Int. J. Heat Mass Transfer 52 (2009) 516;
(c) R.E. Critoph, Z. Tamainot-Telto, S.J. Metcalf, Int. J. Refrig. 32 (2009) 1212;
(d) J.V. Veselovskaya, R.E. Critoph, R.N. Thorpe, S. Metcalf, M.M. Tokarev, Yu.I. Aristov, Appl. Therm. Eng. 30 (2010) 1188.
[40] Y.-K. Seo, J.W. Yoon, J.S. Lee, Y.K. Hwang, C.-H. Jun, J.-S. Chang, S. Wuttke, P. Bazin, A. Vimont, M. Daturi, S. Bourrelly, P.L. Llewellyn, P. Horcajada, C. Serre, G. Férey, Adv. Mater. 24 (2012) 806.
[41] J. Jänchen, D. Ackermann, H. Stach, W. Brösicke, Sol. Energy 76 (2004) 339.
[42] E. Ng, S. Mintova, Microporous Mesoporous Mater. 114 (2008) 1.
[43] S.K. Henninger, F.P. Schmidt, H.-M. Henning, Appl. Therm. Eng. 30 (2010) 1692.
[44] (a) L. Hamon, C. Serre, T. Devic, T. Loiseau, F. Millange, G. Férey, G. De Weireld, J. Am. Chem. Soc. 131 (2009) 8775;
(b) P.L. Llewellyn, S. Bourrelly, C. Serre, A. Vimont, M. Daturi, L. Hamon, G. De Weireld, J.-S. Chang, D.-Y. Hong, Y.K. Hwang, S.H. Jhung, G. Férey, Langmuir 24 (2008) 7245;
(c) A. Vimont, J.-M. Goupil, J.-C. Lavalley, M. Daturi, S. Surblé, C. Serre, F. Millange, G. Férey, N. Audebrand, J. Am. Chem. Soc. 128 (2006) 3218.
[45] G. Férey, C. Mellot-Draznieks, C. Serre, F. Millange, J. Dutour, S. Surble, I. Margiolaki, Science 309 (2005) 2040.
[46] G. Férey, Dalton Trans. 23 (2009) 4400.
[47] G. Férey, C. Serre, Chem. Soc. Rev. 38 (2009) 1380.
[48] P. Küsgens, M. Rose, I. Senkovska, H. Fröde, A. Henschel, S. Siegle, S. Kaskel, Microporous Mesoporous Mater. 120 (2009) 325.
[49] G. Férey, C. Serre, C. Mellot-Draznieks, F. Millange, S. Surblé, J. Dutour, I. Margiolaki, Angew. Chem., Int. Ed. 43 (2004) 6296.
[50] P. Horcajada, S. Surblé, C. Serre, D.-Y. Hong, Y.-K. Seo, J.-S. Chang, J.-M. Grenèche, I. Margiolaki, G. Férey, Chem. Commun. 27 (2007) 2820.
[51] C. Volkringer, D. Popov, T. Loiseau, G. Férey, M. Burghammer, C. Riekel, M. Haouas, F. Taulelle, Chem. Mater. 21 (2009) 5695.
[52] Z. Wang, S.M. Cohen, Chem. Soc. Rev. 38 (2009) 1315.
[53] S. Bernt, V. Guillerm, C. Serre, N. Stock, Chem. Commun. 47 (2011) 2838.
[54] Y.K. Hwang, D.-Y. Hong, J.-S. Chang, S.H. Jhung, Y.-K. Seo, J. Kim, A. Vimont, M. Daturi, C. Serre, G. Férey, Angew. Chem. 120 (2008) 4212.
[55] A. Vimont, H. Leclerc, F. Maugé, M. Daturi, J.-C. Lavalley, S. Surblé, C. Serre, G. Férey, J. Phys. Chem. C 111 (2007) 383.
[56] H. Leclerc, A. Vimont, J.-C. Lavalley, M. Daturi, A.D. Wiersum, P.L. Llwellyn, P. Horcajada, G. Férey, C. Serre, Phys. Chem. Chem. Phys. 13 (2011) 11748.
[57] C. Volkringer, H. Leclerc, J.-C. Lavalley, T. Loiseau, G. Férey, M. Daturi, A. Vimont, J. Phys. Chem. C 116 (2012) 5710.
[58] L. D Gelb, K.E. Gubbins, R. Radhakrsihan, M. Sliwinska-Bartowiak, Rep. Prog. Phys. 62 (1999) 1573.
[59] N.A. Sedron, J.P.R.B. Walton, N. Quirke, Carbon 27 (1989) 853.
[60] A. Vishnyakov, P. Ravikovitch, A.V. Neimark, Langmuir 16 (2000) 2311.
[61] K. Krishnan, R.A. Plane, Inorg. Chem. 5 (1966) 852.
[62] D.A. Young, T.B. Freedman, E.D. Lipp, L.A. Nafie, J. Am. Chem. Soc. 108 (1986) 7255.
[63] A.L. Buck, J. Appl. Meteorol. 20 (1981) 1527.
[64] D. Bolton, Mon. Weather Rev. 180 (1980) 1046.
[65] (a) P.M. Schoenecker, C.G. Carson, H. Jasuja, C.J.J. Flemming, K.S. Walton, Ind. Eng. Chem. Res. 51 (2012) 6513;
(b) G.E. Cmarik, M. Kim, S.M. Cohen, K.S. Walton, Langmuir 28 (2012) 15606;
(c) H. Jasuja, J. Zang, D.S. Sholl, K.S. Walton, J. Phys. Chem. C 116 (2012) 23526.
[66] A. Ristić, N.Z. Logar, S.K. Henninger, V. Kaučič, Adv. Funct. Mater. 22 (2012) 1952.